IOP Publishing

Smart Materials and Structures

Smart Mater. Struct. **31** (2022) 035008 (10pp)

https://doi.org/10.1088/1361-665X/ac4ba8

Shape memory polymer foam: active deformation, simulation and validation of space environment

Lan Luo[1], Fenghua Zhang[1], Wei Pan[1], Yongtao Yao[1], Yanju Liu[2] and Jinsong Leng[1,*]

[1] Centre for Composite Materials and Structures, Harbin Institute of Technology (HIT), Harbin 150080, People's Republic of China

[2] Department of Astronautical Science and Mechanics, Harbin Institute of Technology (HIT), Harbin 150001, People's Republic of China

E-mail: lengjs@hit.edu.cn

Received 25 May 2021, revised 18 August 2021

Accepted for publication 14 January 2022

Published 31 January 2022

Abstract

Shape memory polymer foam (SMPF) is being studied extensively as potential aerospace materials as they have high compression ratio, high specific strength and high specific modulus compared to other shape memory polymers. In this paper, a composite foam with shape memory epoxy as matrix and polyurethane as functional phase was prepared. The SMPF has been characterized by different analytical and testing methods, and its chemical crosslinking reaction and material properties have been studied. The SMPF was installed in the shape memory polymer composite (SMPC) flexible solar array system (SMPC-FSAS), and ground environment tests and orbital validation were performed. Considering the particularity of space environment, the thermal performance test of ground space environment can effectively test the reliability of shape memory performance. Finally, the SMPC-FSAS carried on SJ-20 satellite successfully deployed on geosynchronous orbit for the first time in the world. Moving forward, SMPF assesses the feasibility of applications in the space field and provides more valuable information.

Keywords: shape memory polymers, epoxy foams, space environment simulation, on-orbit validation

(Some figures may appear in color only in the online journal)

1. Introduction

Shape memory polymer foam (SMPF) has the characteristics of low density, high compression ratio and shape memory effect. Consequently, it has research value in many aspects, such as biomedicine and aerospace applications and obtains practical verification [1–3]. In biomedicine, SMPF has good biocompatibility and may be used for tumor implantation therapy by using their shape memory effect and volume expansion rate [4, 5]. In aerospace, its high compression ratio and fixed compression deformation are used to save storage space [6–9]. Using its shape memory effect, it can be stimulated to recover its shape, complete preset functions or drive other devices [10–13]. In textile, SMPF is used as a temperature sensitive filling material to produce lightweight textiles that are insulated at high temperatures [14].

In 2004, Tobushi *et al* [15] made an experimental study on the thermodynamic properties of polyurethane (PU) SMPFs and the effect of environmental conditions on their shape recovery. Huang *et al* [16] proposed a method to study the thermodynamic behavior of SMP PU foam, including the compression test of foam mechanical properties, the free recovery test of shape memory behavior and the constraint recovery

* Author to whom any correspondence should be addressed.

test. Simkevitz *et al* [17] investigated the influence of cell morphology and foam deformation on the shape memory effect of SMPF with foams of different densities. It was found that the change of density has no significant effect on the response time of SMP shape recovery compared with pure SMPF. Wu *et al* [18] studied the shape recovery speed of styrene-based SMP, SMP/carbon black (CB) composite material and SMPF under infrared driving, and found that the shape recovery speed of SMP foam was relatively poor.

Epoxy resins are widely used in the aerospace industry due to their high strength, impact resistance and fatigue resistance. Shape memory epoxy (SMEP) resin is one class of thermosetting polymer. Thermosetting SMPs are a fixed segment with crosslinked phase and a reversible phase with a non-crosslinked phase. The reversible phase may undergo changes of glass state and high reversible elastic state. Generally, shape memory resin systems have fixed permanent crosslinks and reversible phases that can fix shape [19] SMEP foams have also been extensively studied. di Prima *et al* [20–22] mainly studied the mechanical behavior of SMEP foam and established a model to predict foam modulus. Nejad *et al* [23] prepared triple SMEP/polycaprolactone (PCL) composite foam and conducted performance tests. Non-toxic SMPF adapted to the human environment is essential for the treatment of diseases such as biomedical tumors. Shape memory foam can not only meet the conditions of the lightest weight and sufficient structural strength and structural rigidity under certain conditions but also meet the requirements of small space in space transportation. The representative application of SMPF is the wheel of a small Martian rover [24]. The CCSL (CFRF/-CHEM Spring Lock) truss structure composed of SMPF and carbon fiber reinforced polymer is jointly developed by Jet Propulsion Laboratory in the United States [25]. Sokolowski *et al* [6] conducted a space loading experiment of SMEP foam. However, few studies have been done to simulate the spatial environment of shape memory foams. Due to the harshness and complexity of the spatial environment, controlling the behavior of thermal response-driven shape memory is a major challenge. SMPF has the advantages of small space occupied after compression, convenient transportation and storage, and can be used in devices such as space deployment structures. Consequently, it is very necessary to perform a series of spatial environment validation tests on the ground.

In this work, a composite SMEP foam was prepared by blending SMEP resin with soft foam PU. The composite foam material has both the pore structure of the flexible PU foam and the shape memory performance of the SMEP resin. Thermal vacuum test (TVT) and thermal cycle test (TCT) were performed using the parameters obtained from thermal balance, and the effects of the above spatial environment simulation tests on the shape memory performance of SMPF were discussed. Finally, SMPF conducted orbital validation on shape memory polymer composite (SMPC) flexible solar array system (SMPC-FSAS) carried on the SJ-20 geosynchronous satellite.

2. Experimental

2.1. Materials

The self-made SMEP resin in the research group was used as the functional component [26], and the glass transition temperature (Tg) was approximately 150 °C. The commercial flexible PU foam was used as the foaming component. The raw material of flexible PU foam was purchased from Shanghai Shengju Building Materials Co., Ltd, and it was divided into component A and component B. Component A was polyester polyol and other materials, and the component A was an isocyanate material.

2.2. Preparation of SMPF

SMEP resin and PU soft foaming raw material component A were weighed with the same weight, mixed and stirred for 3–4 h. Component B of PU soft foaming material was added into the mixing liquid and poured into the mold. After stirring and foaming, the foam was rested for 30–40 min for normal temperature foaming. The remaining material was put into in the drying chamber of 150 °C blast dryer to cure for 5 h, and then cooled to room temperature naturally. A yellowish foam was obtained after curing, and a cylindrical foam with a diameter of 100 mm was obtained after demoulding. The density of SMPF was measured to be 0.3 g cm^{-3}. The main chemical reactions involved in the synthesis of soft PU foam include the following: gel reaction of polyester or polyether polyols with organic isocyanate toluene diisocyanate, and the gas reaction of water and organic isocyanate [27]. The main physical processes involved include bubble nucleation, bubble growth, microphase separation, aging and polymerization, as shown in figure 1.

2.3. Characterization

2.3.1. Thermal analysis. Fourier transform infrared spectroscopy (FTIR) was used to determine the structure of chemical bonds and functional groups contained in the test sample. The spectrum range during the test was 4000 $\sim$ 400 cm^{-1} with a resolution of 4 cm^{-1}. The thermal weight loss analysis test thermogravimetric analysis (TGA) was performed to investigate the thermal stability of the polymer. Under a nitrogen atmosphere, the temperature increased at a rate of 10 °C min^{-1}. The temperature range was 25 °C–800 °C.

The differential scanning calorimetry (DSC) is used to measures the transition temperature of foam. The DSC thermal analyzer model is DSC/700 of Mettler-Toledo. The temperature was raised in nitrogen at a rate of 10 °C min^{-1} from 25 °C to 180 °C. The second measurement result was taken to eliminate the thermal effect.

Dynamic mechanical thermal analysis (DMA) is a method to measure the change of dynamic mechanical properties of materials in a certain temperature range. The test of composite foam is the shear mode. The test temperature range is

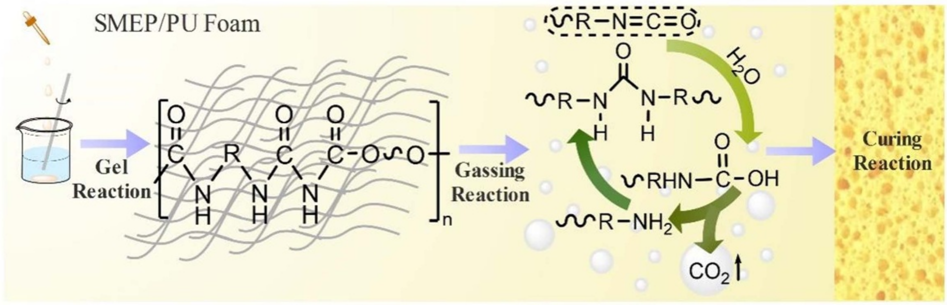

Figure 1. Schematic diagram of the preparation process of SMPF.

−20 °C ~ 130 °C, the heating rate is 5 °C min^{-1}, and the loading frequency is 1 Hz.

2.3.2. Shape-memory behavior. The shape memory effect is a unique performance of SMPF. Shape fixity ratio, recovery ratio and thermomechanical cycle tests of shape memory foams were performed to characterize shape-memory behavior. In this study, SMPF was recovered freely by the thermostatic method and electrothermal film drive method. The shape fixity ratio (R_f) and shape recovery ratio (R_r) of SMPF are calculated as follows:

$$R_\mathrm{f} = \frac{h_0 - h_b}{h_0 - h_a} \times 100\% \tag{1}$$

$$R_\mathrm{r} = \frac{h_t}{h_{0a}} \times 100\% \tag{2}$$

where h_0 is the initial height without compression deformation, h_a is the height with load removed after compression, h_b is the height measured after compression, and h_t is the height after recovery.

2.3.3. Space environment simulation test. Thermal balance, thermal cycle and thermal vacuum were carried out on the ground to simulate the space environment. Thermal balance test simulates the thermal environment (vacuum, cold and black) on geosynchronous orbit to obtain the thermal balance temperature of SMPF. The thermal vacuum experiments of 6.5 cycles and 18.5 cycles of SMPF were carried out to study the thermal stability of the materials. To ensure safety and reliability, the upper and lower limits of temperature were pulled off by 17 °C based on thermal balance temperature.

3. Results and analysis

3.1. Thermal properties

In the FTIR curve of SMEP, there are double absorption peaks at 3529 and 3443 cm^{-1} (as shown in figure 2(a)), which indicate the presence of unreacted amino (–NH_2) in the epoxy resin. The characteristic peak at 1732 cm^{-1} corresponds to the carbonyl group (C=O). The chemical bonds in SMEP have high bond energy, and their chemical properties are stable as shown in figure 2(a). However, compared with SMEP curves, SMPF had more characteristic peaks at 1599, 1411 and 1109 cm^{-1}, corresponding to ester bond (–COO–) and secondary alcohol bond (C–O), respectively. At 2972 cm^{-1}, the hydroxyl and ether group (C–O–C) absorption peaks appeared simultaneously at 1050 and 1300 cm^{-1}, and carbonyl group (C=O) appeared at 1750 cm^{-1}, which confirm the existence of ester groups. This is because the PU chain generated in the synthesis process of PU constitutes the PU molecular chain. Furthermore, the organic isocyanate reacts with water to form an unstable carbamate, which then decomposes to form amine compounds and carbon dioxide gases, as shown in figure 2(b).

TGA determines the temperature range for the material to be used and explores the thermal stability of the polymer to ensure that the material can work under the most efficient conditions. As shown in figure 2(c), the decomposition end temperature of the composite foam prepared by mixing two resins is about 500 °C, and the thermal stability of the composite foam is not as good as that of the single-component foam. The decomposition temperature range of composite foam was expanded, and the decomposition rate accelerated from about 300 °C. It reached the peak at about 400 °C and ends at 500 °C. Meanwhile, the TGA curve shows that when the ambient temperature is below 200 °C, the composite foam material remains stable without thermal decomposition, and the mass loss can be ignored. Therefore, the best use temperature of composite foam is below 200 °C. The DSC test results show that the glass transition temperature of the SMPF is 108.7 °C, and the Tg of pure PU was 68.4 °C, as shown in figure 2(d). The results show that Tg of SMPF decreased about 30% after adding PU.

3.2. Mechanical properties

Dynamic thermal analysis is mainly used to study the viscoelasticity of materials, which can accurately obtain the glass transition temperature of materials. The Tg of the measured SMPF is 91 °C as shown in figure 3(a). When PU was added to SMEP, the Tg decreased by nearly 50 °C. SMEP and SMPF decrease their modulus by two orders of magnitude from the storage modulus curve as shown in table 1 compared to the modulus at normal and high temperatures. It shows that they have excellent shape memory performance [28]. At the same time, compared with the Tg data of DSC test, both test results

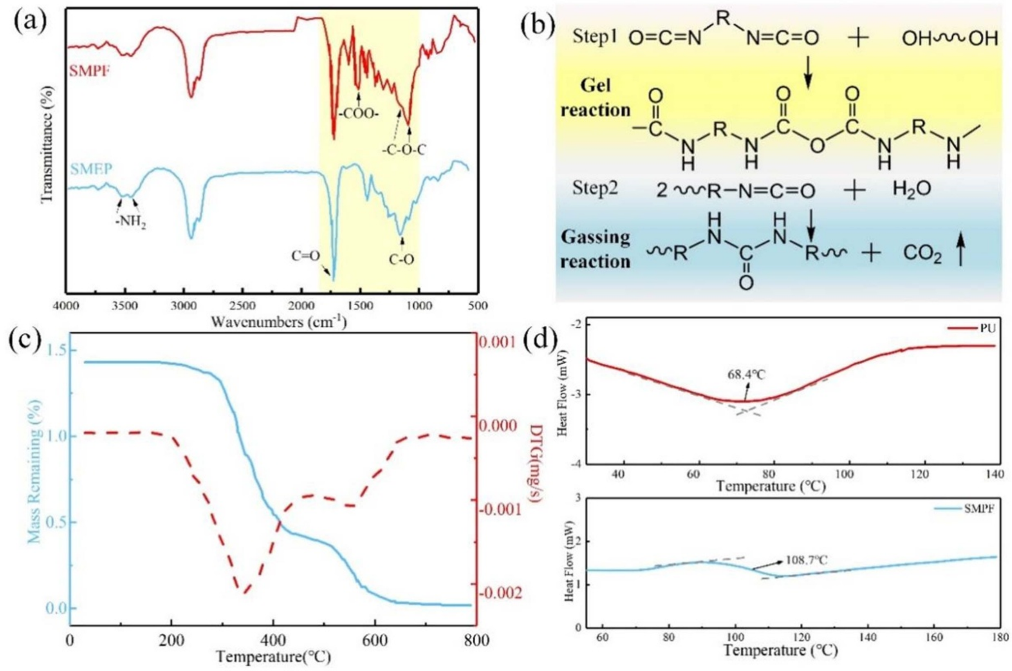

Figure 2. (a) FTIR curve of SMEP and SMPF; (b) reaction equation of SMPF; (c) TGA curve of SMPF; (d) DSC curve of PU and SMPF.

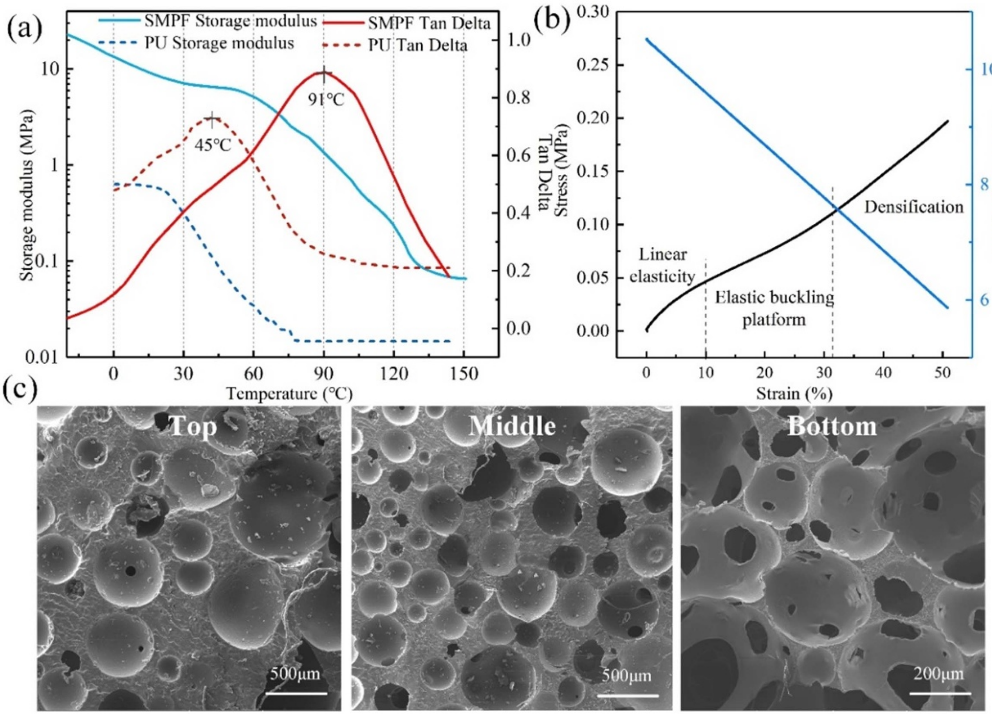

Figure 3. (a) DMA test curve of SMPF; (b) compressive stress–strain curve of SMPF; (c) morphology of SMPF at different positions.

showed that the Tg of PU was 50 °C higher than that of SMPF as shown in table 1. The SMPF has different compressive mechanical properties at different temperatures. The compression curves of SMEP foam composites can be roughly divided into linear elasticity, plateau and densification as shown in figure 3(b). The Ashby–Gibson cross cube foam model is used to explain the relationship between the deformation of the cell and the macroscopic mechanical properties in the compression process [29]. Under unidirectional compression load, when the strain is less than 10%, the holes and ridges of SMPF undergo linear elastic bending. The holes and ridges are the main force-bearing part, and the force is proportional to the displacement. With the increase of pressure, the buckling of the pore wall is the second stage, and the foam hole increases

Table 1. Results of DMA and DSC.

Sample	Tg (°C) (DSC)	Tg (°C) (DMA)	E (Pa) $T = 25$ °C	E (Pa) $T = \mathrm{Tc} + 20$ °C
SMEP	152.9	146	2.26×10^9	1.826×10^6
PU	68.4	45	6.335×10^5	1.469×10^4
SMPF	108.7	91	2.835×10^7	6.485×10^4

E: Storage modulus of DMA test.

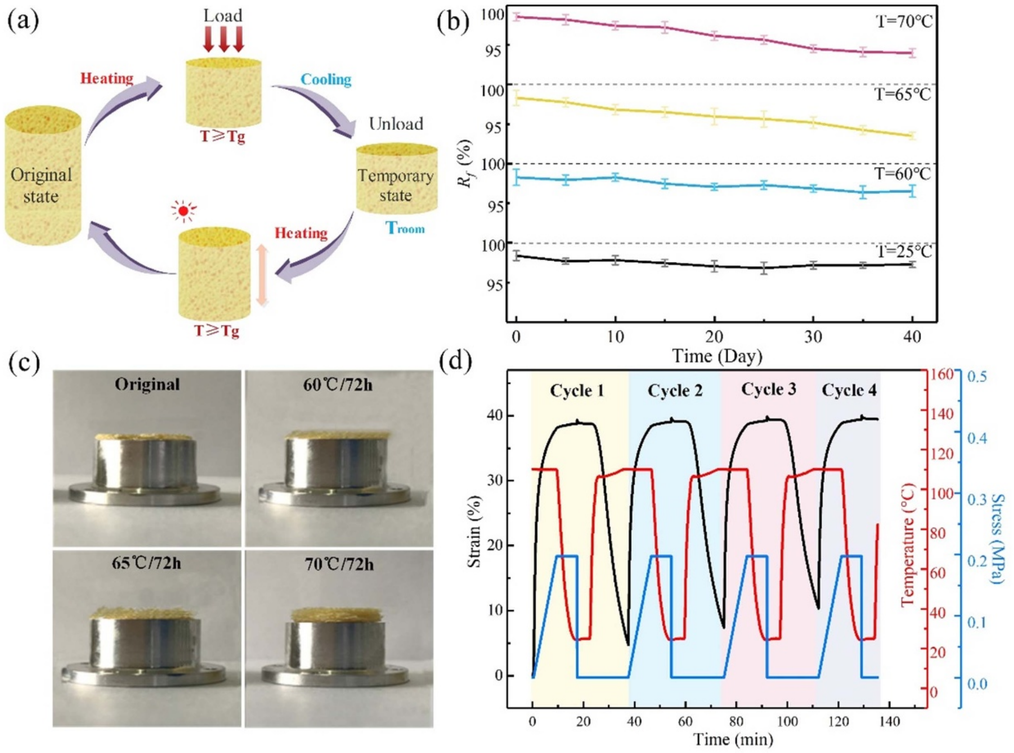

Figure 4. (a) Schematic diagram of the shape memory process; (b) shape memory foam fixity rate; (c) shape memory foam fixity rate experiment result graph. (d) Shape memory cycle of SMPF.

with the increase of compaction density, resulting in instability and elastic buckling [30, 31]. When the foam holes are close to being completely closed, the interior of the foam holes is close to being fully in contact with each other. Scanning electron microscopy was used to observe the microstructure of the SMEP composite foam, as shown in figure 3(c). The pore units of SMPF were relatively uniform, and each macropore unit had many small holes attached to the pore unit. It can be observed that the upper end of the foam was obturator, while the middle and lower parts were even.

3.3. Shape memory performance

Shape fixity ratio and shape recovery ratio are important physical quantities to characterize the shape memory effect of SMPF. After adding PU to SMEP, the shape memory effect of SMPF changed. Shape recovery performance experiments were designed to study changes in SMPF recovery performance near Tg. Each sample with a height of 40 mm was compressed to 10 mm and heated in an oven at 110 °C. Height changes of SMPF are measured with a laser rangefinder and R_f and R_r are calculated as shown in figure 4(a). The shape recovery ratio of epoxy foam under electric heating was tested with a power of 5.6 W and a heating time of 10 min.

Shape fixity is an important physical quantity to investigate the shape memory effect of shape memory materials. To ensure the smooth deployment of SMPF in the space environment, the test temperature was strictly increased to 60 °C, which was 17 °C higher than the actual environment temperature. SMPF was compressed to 10 mm at 100 °C and then maintained pressure to fix shape until cooled to room temperature. The height of the foam was recorded for 40 d at different temperatures, and then the fixity ratio was calculated. The results show that SMPF exhibited excellent shape fixity (more than 95%) when the temperature was between 60 °C to 70 °C, the speed of shape recovery slowed down over time, but the amplitude was small. After that, when a stable state is reached and there is little shape recovery, the internal stress of the material is balanced and the shape is completely fixed. Height was measured after SMPF compression was fixed and shape was restored, respectively, and shape

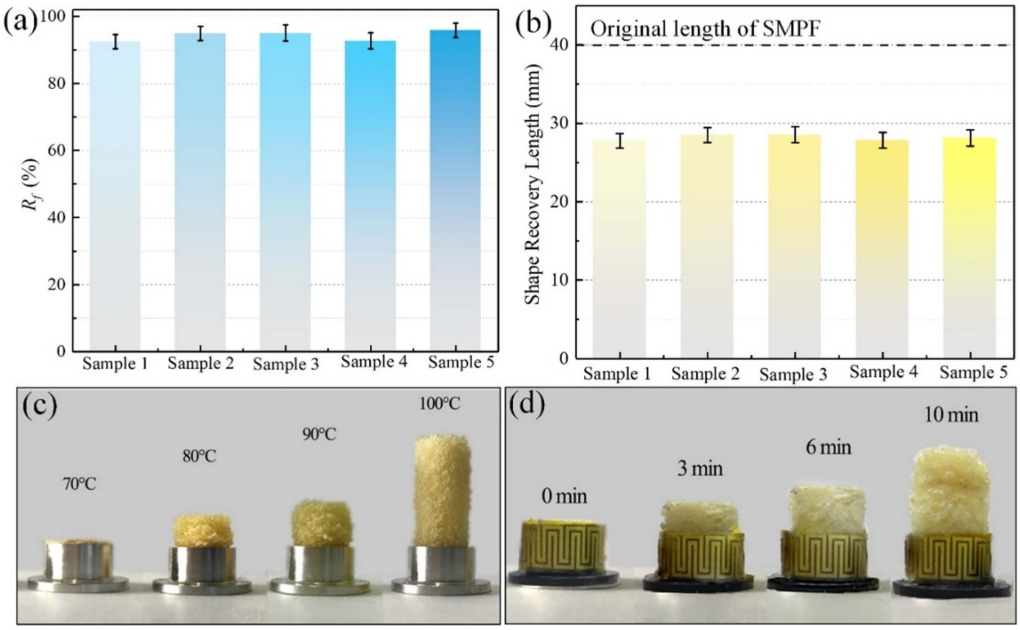

Figure 5. (a) Shape fixity rate of SMPF; (b) electrically heated SMPF shape recovery height; (c) shape recovery process of SMPF; (d) electric heating shape recovery process of SMPF.

recovery rates were calculated from equations (1) and (2) recorded. The shape fixity ratio is almost constant, that is, the shape of the SMP is completely fixed. The results of the shape memory fixation test and the error bars of the four experiments are shown in figure 4(b). The errors may be due to the inability of the measurement to achieve infinite accuracy and the conduction of the ambient temperature. As can be seen from figure 4(c), when the temperature reached 70 °C, the foam somewhat recovered compared with the original state, but generally achieved an ideal shape fixity. This is due to the mixing of soft foamed PU, which causes excessive internal stress in the material during large deformation. The storage stress of the hard chain segment in SMPF was not enough to maintain shape, and the shape recovery increased. In conclusion, SMPF can show excellent shape-fixing performance at 60 °C and meet the space environmental requirements.

Ensure temperature and stress cycles, and measure strain changes. Equations (1) and (2) were used to calculate R_f and R_r for each cycle according to the strain curve. The R_f for the 1st cycle, 2nd cycle, and 3rd cycle are 99.5%, 99.2% and 99.1%, respectively. Meanwhile, the R_r for the 1st cycle, 2nd cycle, and 3rd cycle are 95.5%, 92.6% and 89.6%, respectively [32]. Compression cycling test of SMPF was performed by DMA test, and four consecutive shape memory cycling processes were performed by editing program. In four consecutive thermal cycles, the relationship between shape fixation rate, shape recovery rate and cycle times is discussed. Figure 4(d) shows the relationship between strain, stress, temperature, and time during the compression thermal cycle of SMPF. In the compression thermal cycling experiment, the recovery ratio of SMPF decreased slightly with the increase of the number of shape memory cycles. The maximum compression strain, shape memory fixity ratio and recovery ratio change little with the number of shape memory cycles.

Shape recovery performance experiments were designed to investigate the recovery performance of SMPF near Tg. Especially, when PU was added to SMEP, the shape memory effect of SMPF changed. To simulate deployment on orbit, a heating film was used to drive the foam. The temperature chamber and heating film driving methods were used to test the shape recovery performance of the foams. For stability and reliability, each sample was tested 20 times. The results in figure 5(a) show that the response rate of each sample repeated 20 times is greater than 95%, and the deployed SMPF is shown in figure 5(c). The shape recovery rate of each sample was tested 20 times, and the performance stability of SMPF was proved. On the other hand, due to the gap between the electric heating film and the foam, SMPF can be extended from 10 to 30 mm in 10 min, as shown in figures 5(b)–(d). From the comparison of figures 5(c) and (d), it can be seen that the electro-heated membrane method does not allow SMPF to be fully expanded at the expense of its expansion height. At the same time, due to the pore structure of the foam itself, it cannot conduct heat from bottom to top. Ultimately, the shape recovery rate of the original length of the 40 mm SMPF can reach 70%–80% utilizing the electric heating film. When the foam deploys beyond the height of the electric heating film, it needs to rely on its own heat transfer for shape recovery, which prolongs the recovery time.

4. Ground test validation

4.1. Thermal balance test

The thermal balance test was carried out in the KFTA solar simulator, including vacuum, cold black environment. It is used to test the temperature distribution and the function of spacecraft thermal control system under the orbit flight

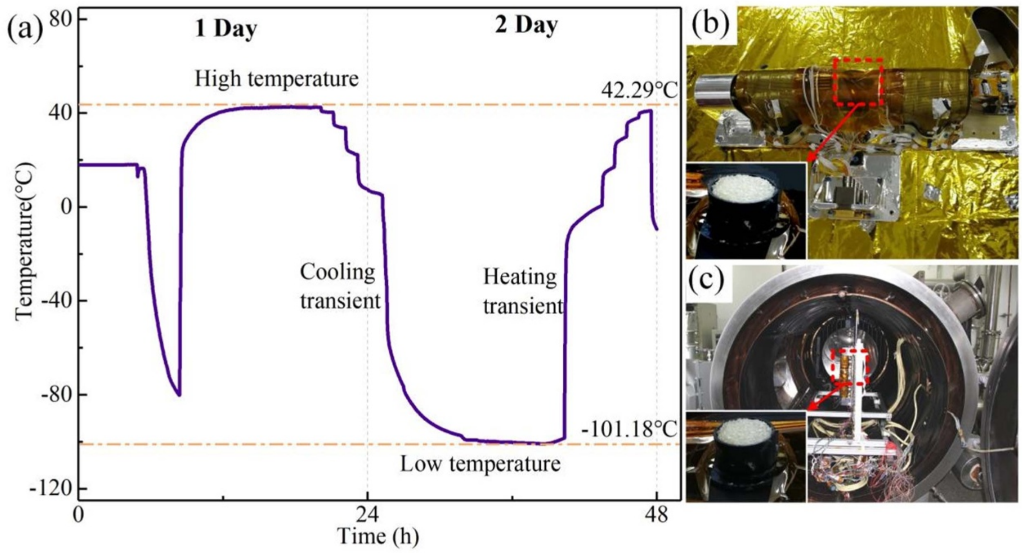

Figure 6. (a) Thermal balance test curve; (b) pre-test state; (c) post-test state.

equilibrium state. After compressed state of SMPF was stabilized, thermal balance tests were performed on SMPC-FSAS as shown in figure 6(b). Generally speaking, it is based on the orbital cycle of the spacecraft, and the test conditions include high and low temperature conditions, as shown in figure 6(a). The experiment was carried out using the solar simulator, and the state after the thermal balance test as shown figure 6(c). SMPF remained compressed state, indicating that SMPF cannot be recovered in a space environment. In vacuum, there are only two ways of heat transfer: heat radiation and heat conduction. Thermal equilibrium experiments provide heat flow simulations corresponding to sunlight and incident angles. The thermal radiation provided by the solar simulator has good collimation, uniformity and stability, which is consistent with the space thermal environment. As shown in figure 6(a), the highest temperature can reach 42.29 °C and the lowest can reach -101.18 °C. At the same time, according to the shape fixity ratio shown in figure 4(b), it can be demonstrated that the shape of SMPF can be accurately fixed in space, and the space thermal environment has little effect on it. In other words, SMPF can always remain compressed state in a spatial environment without issuing the deployment command.

4.2. Thermal vacuum test (TVT)

TVT is a kind of thermal environment test that verifies or inspects spacecraft product functions, inspects spacecraft manufacturing processes, and discovers early failures of spacecraft equipment under vacuum and specified temperature cycling conditions. From room temperature to the lowest temperature for cold soaking, then to the highest temperature for hot soaking, and finally back to room temperature, it becomes a temperature cycle. According to the heat balance test, the temperature range of SMPF is -101.18 °C $\sim$ 42.29 °C. In order to improve the reliability and safety, the temperature of TVT is widened to -120 °C $\sim$ 90 °C, and 6.5 cycles are performed as shown in figure 7(a). The TVT is to verify that the SMPF can withstand the predicted extreme temperature under vacuum and extreme temperature conditions, while also verifying the SMPF's ability to withstand temperature cycling stress. In thermal vacuum experiments, it is observed that SMPF has recovered after the first cycle. SMPF showed no sign of slagging after the test and completed the recovery process within 10 min as shown in figure 7(c). The compressed state before the SMPF TVT and the deployment state after the test are shown in figure 7(d). It is proved that the performance of the SMPF after TVT was not affected. In order to verify the effect of thermal vacuum experiment on SMPF, the shape recovery ratio of two samples without thermal vacuum experiment (I) and after thermal vacuum experiment (II) were tested, as shown in figure 7(b). It is found that the trend of shape recovery ratio was almost the same for samples I and II at different temperatures, indicating that the thermal vacuum has little effect on the shape memory performance of SMPF.

4.3. Thermal cycling test

The TCT was carried out to improve the reliability of the components. The potential material and manufacturing quality defects in the products are exposed in the early stage, the early failure is eliminated, and the reliability of the products is improved. The thermal cycle temperature measurement is set according to the thermal balance test. The range of -101.18 °C $\sim$ 42.29 °C is obtained by simulating thermal radiation through the thermal balance test. In order to ensure the safety and reliability of on orbit experiment, the upper and lower deflection temperatures are reduced to -120 °C $\sim$ 90 °C. The TCT was repeated alternating high and low temperatures. When maintaining high and low temperature, the time of each temperature maintaining stage is 8 h. The temperature holding time meets the satellite's requirements for on-orbit operating conditions and working mode

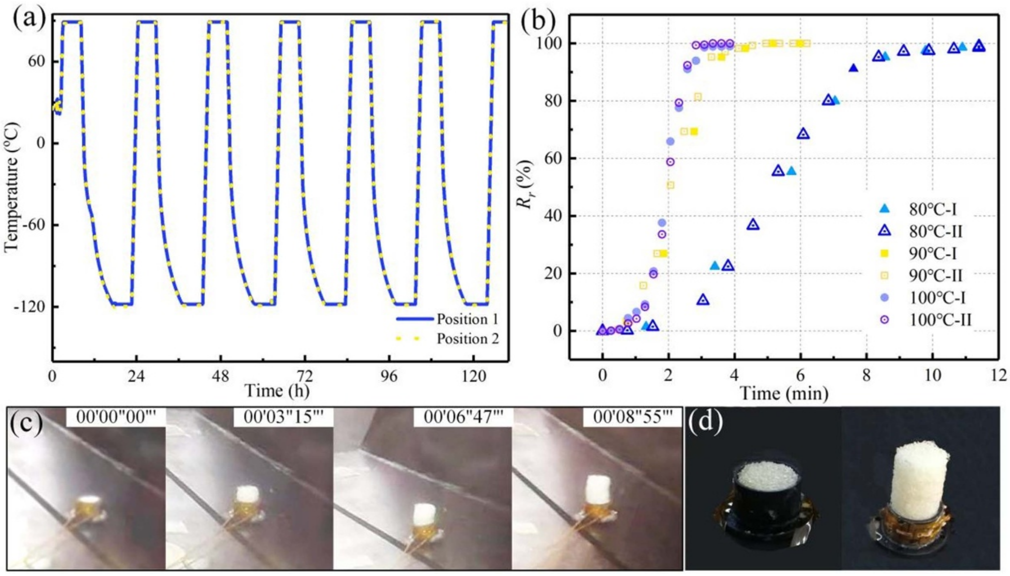

Figure 7. (a) Thermal-vacuum test curve; (b) shape memory performance comparison; (c) thermal-vacuum test process (d) SMPF thermal-vacuum test before and after comparison.

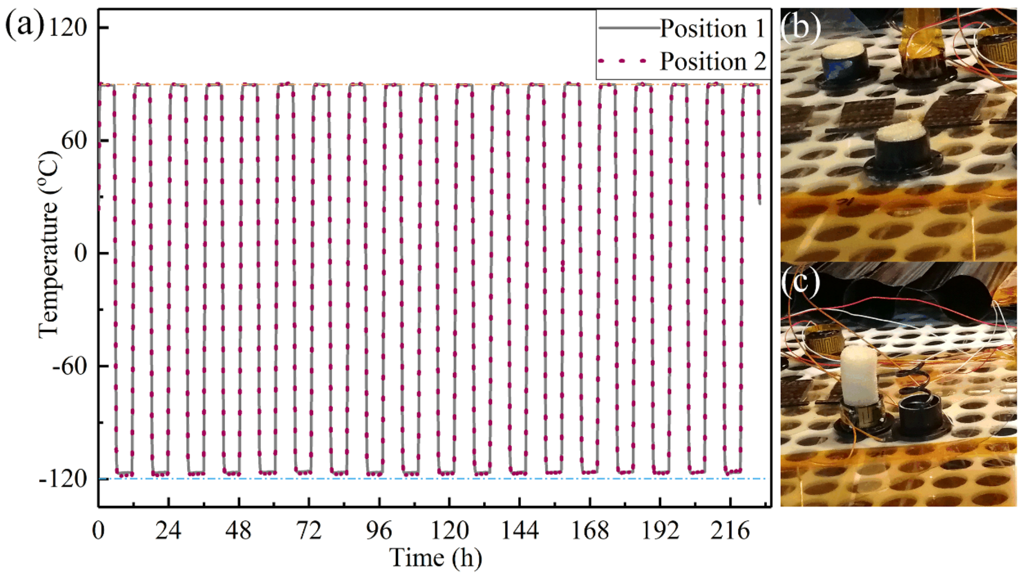

Figure 8. (a) TCT curve; (b) compression state of SMPF TCT; (c) expanded state of SMPF TCT.

tests. The test has undergone a total of 18.5 cycles as shown in figure 8(a). According to the test results, SMPF was fully recovered in 10 min during the first TCT. SMPF did not change during the subsequent 18.5 temperature cycles, as shown in figure 8(c). The temperature of each cycle is from low temperature (−120 °C) to high temperature (90 °C) and maintained for 8 h. The foam remained compressed state during the thermal cycle. To verify the effect of temperature cycling on SMPF, the samples after the thermal cycle were conducted out for shape memory performance testing. The shape memory properties of four samples were tested. The results show that the shape fixity ratio and shape recovery ratio had little change before and after thermal cycling test, indicating that thermal cycling had no effect on the shape memory performance of SMPF.

5. On-orbit demonstration

The SMPC-FSAS carried on the SJ-20 Geostationary Satellite was successfully launched on a Long March 5 Y3 heavy-lift rocket from the Wenchang Satellite Launch Center on 27 December 2019. And the world's first SMPC-based flexible solar array (shown in figure 9(b)) was deployed on 5 January 2020. Figure 9(a) depicts the track temperature curves of SMPF under compression and deployment states. At stage I, the temperature of the SMPF surface was 65 °C (figure 9(a)) and the SMPF remained compressed state until the deployment test was carried out the second day after entering the synchronous orbit (stage II). The locking function of the SMPC release mechanism of SMPC-FSAS was in a normal state during the launch process. The foam was compressed and

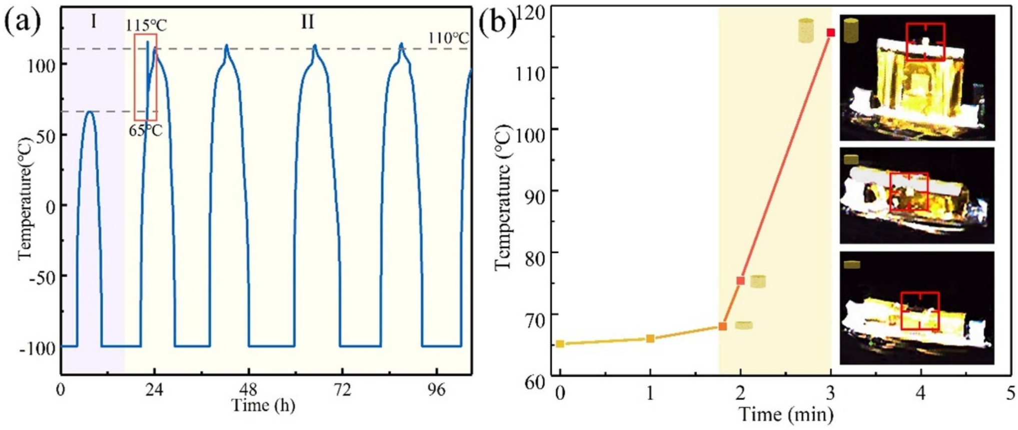

Figure 9. (a) On-orbit temperature curve; (b) on-orbit deployment verification. Reprinted by permission from Springer Nature Customer Service Centre GmbH: Journal Publisher Springer Nature, Science China Technological Sciences [33], Copyright © 2020, Science China Press and Springer-Verlag GmbH Germany, part of Springer Nature.

placed in the hole. The configuration of SMPF during deployment is shown in figure 9(b). The surface temperature of SMPF raised sharply during heating because it was also exposed to the direct surface temperature of sunlight, thus reaching 110 °C. As shown in the green box in figure 9(a), the unfolding process of SMPF was completed from 65 °C to 115 °C. The curve in figure 9(b) shows the monitoring process of surface temperature change and shape recovery of SMPF in orbit. There was no slag during the recovery process, and the recovery process was completed in 60s.

6. Conclusions

In this paper, a SMEP composite foam with open-hole structure was prepared, which was based on SMEP resin and used soft PU foam as foaming material. Controlling the shape memory behavior of thermal-responsive SMPs is a challenge due to the severe and complex space environment. The temperature boundary of the material under space environmental conditions was obtained from the thermal balance test of SMPF. Thermal vacuum and thermal cycling tests were then performed to simulate and evaluate the thermomechanical properties of the material in space. Ground environment simulation and orbital validation results show that SMPF driven by electric heating membrane can meet the temperature requirements of vacuum and atmospheric environment. It is worth mentioning that SMPF showed excellent shape memory performance both on the ground and in space. The shape fixing rate remains basically 99%. SMPF enables rapid expansion within 60 s by heat transfer from the electrothermal film. The SMPF has light-weight, large compression-deployment ratio, simple and reliable deployment drive, and has important potential application value in space engineering.

Data availability statement

All data that support the findings of this study are included within the article (and any supplementary files).

Acknowledgments

This work is supported by the National Natural Science Foundation of China (Grant No. 11632005). The authors would like to thank for the direction and help from Institute of Telecommunication Satellite, China Academy of Space Technology (CAST).

ORCID iDs

Yanju Liu https://orcid.org/0000-0001-8269-1594
Jinsong Leng https://orcid.org/0000-0001-5098-9871

References

[1] Li G and Muthyala V D 2008 Impact characterization of sandwich structures with an integrated orthogrid stiffened syntactic foam core *Compos. Sci. Technol.* **68** 2078–84
[2] Xu T and Li G 2011 A shape memory polymer based syntactic foam with negative Poisson's ratio *Mater. Sci. Eng.* A **528** 6804–11
[3] Xu T and Li G 2011 Durability of shape memory polymer based syntactic foam under accelerated hydrolytic ageing *Mater. Sci. Eng.* A **528** 7444–50
[4] Small W I V *et al* 2009 Magnetic resonance flow velocity and temperature mapping of a shape memory polymer foam device *Biomed. Eng. Online* **8** 42
[5] Ortega J *et al* 2007 Vascular dynamics of a shape memory polymer foam aneurysm treatment technique *Ann. Biomed. Eng.* **35** 1870–84
[6] Sokolowski W M and Hayashi S 2003 *Smart Structures and Materials 2003: Smart Structures and Integrated Systems* vol 5056, ed A M Baz pp 534–44
[7] Perkins D A, Reed J L and Havens E 2004 *Smart Structures and Materials 2004: Industrial and Commercial Applications of Smart Structures Technologies* vol 5388, ed E H Anderson pp 225–33
[8] Santo L *et al* 2013 Mission STS-134: results of shape memory foam experiment *Acta Astronautica* **99** 333–40
[9] Sokolowski W, Tan S, Willis P and Pryor M 2008 Shape memory self-deployable structures for solar sails *Smart*

Materials V vol 7267, ed N H Voelcker and H W Thissen (https://doi.org/10.1117/12.814301)
[10] Rodriguez J N *et al* 2014 *In vivo* response to an implanted shape memory polyurethane foam in a porcine aneurysm model *J. Biomed. Mater. Res.* A **102** 1231–42
[11] Singhal P *et al* 2014 Low density biodegradable shape memory polyurethane foams for embolic biomedical applications *Acta Biomater.* **10** 67–76
[12] Landsman T L *et al* 2017 A shape memory foam composite with enhanced fluid uptake and bactericidal properties as a hemostatic agent *Acta Biomater.* **47** 91–99
[13] Wang J *et al* 2019 Development of shape memory polymer nanocomposite foam for treatment of intracranial aneurysms *Mater. Lett.* **250** 38–41
[14] Chung Y-C, Cho T K and Chun B C 2009 Flexible cross-linking by both pentaerythritol and polyethyleneglycol spacer and its impact on the mechanical properties and the shape memory effects of polyurethane *J. Appl. Polym. Sci.* **112** 2800–8
[15] Tobushi H, Matsui R, Hayashi S and Shimada D 2004 The influence of shape-holding conditions on shape recovery of polyurethane-shape memory polymer foams *Smart Mater. Struct.* **13** 881–7
[16] Huang W M, Lee C W and Teo H P 2006 Thermomechanical behavior of a polyurethane shape memory polymer foam *J. Intell. Mater. Syst. Struct.* **17** 753–60
[17] Simkevitz S and Naguib H 2007 Effects of density and cell morphologies on the shape memory effect of a porous shape memory polymer *SPIE Smart Structures and Materials + Nondestructive Evaluation and Health Monitoring* (*San Diego, California, United States, 27 April 2007*) vol 6525, Y Matsuzaki, M Ahmadian and D J Leo (https://doi.org/10.1117/12.715443)
[18] Wu X, Liu Y and Leng J 2008 Study on shape recovery speed of SMP, SMP composite, and SMP foam *SPIE Smart Structures and Materials + Nondestructive Evaluation and Health Monitoring,* (*San Diego, California, United States, 26 March 2008*) vol 6931, V K Varadan (https://doi.org/10.1117/12.775955)
[19] Zhao Q, Qi H J and Xie T 2015 Recent progress in shape memory polymer: new behavior, enabling materials, and mechanistic understanding *Prog. Polym. Sci.* **49–50** 79–120
[20] di Prima M *et al* 2010 Deformation of epoxy shape memory polymer foam. Part I: experiments and macroscale constitutive modeling *Mech. Mater.* **42** 304–14
[21] di Prima M A *et al* 2010 Deformation of epoxy shape memory polymer foam: part II. Mesoscale modeling and simulation *Mech. Mater.* **42** 315–25
[22] di Prima M A *et al* 2007 Thermo-mechanical behavior of epoxy shape memory polymer foams *Smart Mater. Struct.* **16** 2330–40
[23] Nejad H B, Baker R M and Mather P T 2014 Preparation and characterization of triple shape memory composite foams *Soft Matter* **10** 8066–74
[24] Sokolowski W M and Tan S C 2007 Advanced self-deployable structures for space applications *J. Spacecr. Rockets* **44** 750–4
[25] Sokolowski W, Seng T and Pryor M 2004 Lightweight shape memory self-deployable structures for gossamer applications *The 45th AIAA/ASME/ASCE/AHS/ASC Structures, Structural Dynamics & Materials Conf.* vol 4 pp 19–22
[26] Leng J, Wu X and Liu Y 2009 Effect of a linear monomer on the thermomechanical properties of epoxy shape-memory polymer *Smart Mater. Struct.* **18** 756–7579
[27] Chung S E and Park C H 2010 The thermoresponsive shape memory characteristics of polyurethane foam *J. Appl. Polym. Sci.* **117** 2265–71
[28] Tang L *et al* 2020 Enhanced toughness and mechanical property of epoxy resins with good shape memory behaviors *Fibers Polym.* **21** 1187–94
[29] Xiao Z *et al* 2018 Evaluation of topology-optimized lattice structures manufactured via selective laser melting *Mater. Des.* **143** 27–37
[30] Xu B *et al* 2010 Thermal-mechanical properties of polyurethane-clay shape memory polymer nanocomposites *Polymers* **2** 31–39
[31] Lei M *et al* 2016 Micro-mechanics of nanostructured carbon/shape memory polymer hybrid thin film *Soft Matter* **12** 106–14
[32] Li W, Liu Y and Leng J 2017 Programmable and shape-memorizing information carriers *ACS Appl. Mater. Interfaces* **9** 44792–8
[33] Lan X *et al* 2020 World's first spaceflight on-orbit demonstration of a flexible solar array system based on shape memory polymer composites *Sci. China-Technol. Sci.* **63** 1436–51